

A Comprehensive Study of Adjoint-Based Optimization of Non-Linear Systems with Application to Burgers' Equation

Alexandru Fikl, Vincent Le Chenadec, Taraneh Sayadi

University of Illinois at Urbana-Champaign, Aerospace Engineering Department, United States

Peter J. Schmid

Department of Mathematics, Imperial College London, United Kingdom

In the context of adjoint-based optimization, nonlinear conservation laws pose significant problems regarding the existence and uniqueness of both direct and adjoint solutions, as well as the well-posedness of the problem for sensitivity analysis and gradient-based optimization algorithms. In this paper we will analyze the convergence of the adjoint equations to known exact solutions of the inviscid Burgers' equation for a variety of numerical schemes. The effect of the non-differentiability of the underlying approximate Riemann solver, complete vs. incomplete differentiation of the discrete schemes and inconsistencies in time advancement will be discussed.

I. Introduction

Adjoint methods have been traditionally used in flow and design optimization (with seminal papers by Pironneau [1] and Jameson [2]) and sensitivity analysis, generally for linear equations, continuous flow variables or numerical models that regularize shocks in some way (steady-state RANS models, artificial viscosity, etc.). In the field of fluid mechanics, adjoint methods are of particular interest because they drastically reduce the size of the problem by using the *adjoint equations* instead of differentiation techniques to compute the derivatives of a given cost functional (see [3] for a general introduction to flow control). Optimization problems with PDE-based constraints have been the focus of significant research, see, for example, [4, 5] for a study with an emphasis on elliptic/parabolic equations, and [6] for a view

on hyperbolic equations as optimization constraints. Less often studied, but still of great importance, are applications that require the use of nonlinear PDEs with highly localized features (reactive zones), large gradients (boundary layers), discontinuities (shocks) or interfaces (multiphase flows). These complexities, which could even arise for well-behaved initial data, pose significant problems to the existence and uniqueness of a solution to the state and the adjoint equations, which can have tremendously negative effects on the convergence of any optimization algorithm.

The issues of adjoint optimization in the context of nonlinear conservation laws with shocks have been studied numerically to a large extent in the past (see [7, 8, 11]). Non-differentiable optimization techniques, based on subgradients, have been successfully employed to solve such problems [15]. There have also been attempts at using methods which do not rely on the gradient information, such as stochastic optimization [9] or genetic algorithms [12]. However, these methods also suffer from limitations, usually related to very high computational costs compared to classical gradient descent methods.

Despite the importance of problems involving some kind of discontinuity in the flow variables, little attention has been placed on the existence and uniqueness or the consistency and convergence of the continuous or discrete equations, respectively. Recent contributions such as [16, 20] and [18, 19] have formally defined the problems and given proofs of the existence of an optimal control, the pointwise convergence almost everywhere of the linearized and adjoint equations, as well as of the cost functional in the case of scalar conservation laws. These proofs have been extended to cases with Dirac initial data and multiple shocks and provide a solid basis for future analysis. Another approach that has received attention is the possibility of adding the shock locations as independent variables to the existing set of equations [13], and developing specialized descent algorithms that use this information [23]. Entirely new numerical methods that explicitly track the shock location may be required as well, which could be too complex to be practical in some cases (see also the work on front-tracking in [10]).

In this paper, we propose to perform extensive numerical studies on various discrete schemes for nonlinear conservation laws and provide insights into their convergence (if possible) in different scenarios. This follows the numerical work done in [18, 19] on a linear modified Lax-Friedrichs scheme, where convergence has been formally proven for both the linearized equations and the adjoint equations. However, the analytical work done by Giles and Ulbrich is extremely difficult to extend to more advanced nonlinear numerical schemes, given the current corpus of knowledge in the field of stability and convergence analysis. Thus, we propose rigorous numerical testing to gain insight into the behavior of widely used nonlinear numerical schemes.

There are many issues that can be investigated in this area. Firstly, we will investigate

the time discretization of the adjoint equations, as obtained by taking the transpose of the linearized discrete operators. When discretizing the continuous adjoint equations, it is unclear at what time the state variables that appear in nonlinear schemes should be taken, e.g. t^m, t^{m+1} or some intermediate level in multi-stage time integration. This issue will be discussed in Section III in the case of discrete adjoint equations, which should shed light on the continuous case as well.

We will also look, in Section IV, at the spatial discretization and see what impact non-differentiable approximate Riemann solvers will have on the convergence of the numerical schemes. This issue is mostly of relevance when automatic differentiation software is not used and the discrete equations are differentiated manually. It has been suggested in [22] that incomplete differentiation has very little impact on the end results (for the Euler equations with a Roe flux).

Following these investigations, in Section V, we will use the modified Lax-Friedrichs scheme proposed in [18, 19] to construct a hybrid numerical scheme that uses a second order flux limited scheme away from the shocks, resulting in the expected convergence at the shock and high-order accuracy in smooth regions. A major finding by [18, 20] concerning converging schemes, like the modified Lax-Friedrichs scheme, is that they generally require an inherent form of artificial dissipation. The dissipation has the effect of smearing the shock across an increasing number of cells as the grid is refined, thus allowing the numerical scheme to implicitly satisfy the boundary conditions for the adjoint at the shock locations. This remark may also explain why many practical tests that have been done in the past, using artificial viscosity or similar techniques, have been successful to quite a large extent.

II. Adjoint Methods

There are two main branches of adjoint methods in use today: the *differentiate-then-discretize* approach, which derives the continuous adjoint equations from the state equations and discretizes them separately, and the *discretize-then-differentiate* approach, which discretizes the state equations and derives a discrete adjoint that is consistent with the discrete state equations. The first approach is usually preferred because it allows different choices of numerical schemes or even meshes for the state and adjoint equations. This can prove very advantageous, for example, when using adaptively refined meshes, since the state and adjoint variables will have very different areas of interest. A downside to the *differentiate-then-discretize* approach is that, at a discrete level, the obtained gradient is not guaranteed to be consistent, and typically gives rise to numerical instabilities. On the other hand, in the *discretize-then-differentiate* approach, the adjoint equations are obtained from the discrete state equations, and the gradient is guaranteed to be consistent at the discrete level. For a

more general discussion on the trade-offs involved see [3, 33].

Lagrangian Formalism

We will first look at the continuous case and the *differentiate-then-discretize* approach. A common formulation for constrained optimization problems is as follows:

$$\begin{cases} \min_{u,g} \mathcal{J}(u, g), \\ F(u, g) = 0, \\ g \in \mathcal{G}_{\text{ad}}, \end{cases} \quad (1)$$

where u is known as a *state variable*, g is the *control variable*, $F(u, g)$ is a set of (PDE-based) constraints and \mathcal{G}_{ad} is a set of admissible controls. Assuming that the functional \mathcal{J} allows a unique minimizer g^* (see, for example, [4] for very general considerations), one way to solve such a *constrained optimization problem* is to transform it into an unconstrained optimization problem using *Lagrange relaxation* and the Lagrangian functional:

$$\mathcal{L}(u, g, p) = \mathcal{J}(u, g) - \langle p, F(u, g) \rangle,$$

where p is an *adjoint* variable (usually referred to as a Lagrange multiplier) introduced to enforce the constraints $F(u, g)$ and $\langle \cdot, \cdot \rangle$ is an appropriate inner product. If we assume that our variables (u, g) are smooth, we can define the well-known first order necessary conditions for the minimizer of \mathcal{L} :

$$0 = \frac{\partial \mathcal{L}}{\partial p}(u, g, p) = -F(u, g), \quad (2a)$$

$$0 = \frac{\partial \mathcal{L}}{\partial u}(u, g, p) = \frac{\partial \mathcal{J}}{\partial u} - \left(\frac{\partial F}{\partial u} \right)^* p, \quad (2b)$$

$$0 = \frac{\partial \mathcal{L}}{\partial g}(u, g, p) = \frac{\partial \mathcal{J}}{\partial g} - \left(\frac{\partial F}{\partial g} \right)^* p, \quad (2c)$$

which form the *optimality system*, where (2a) retrieves the constraints, (2b) is the adjoint system and (2c) is the so-called optimality condition. We have denoted by $(\cdot)^*$ the adjoint of the given operator. However, the ultimate goal is to find a formula for the derivative of $\mathcal{J}(u(g), g)$ with respect to g and, thus, the sensitivity of the cost functional with respect to each control variable. The chain rule gives:

$$\frac{d\mathcal{J}}{dg} = \frac{\partial \mathcal{J}}{\partial g} + \frac{\partial \mathcal{J}}{\partial u} \frac{du}{dg}. \quad (3)$$

If we differentiate the constraints $F(u(g), g)$, we find:

$$\frac{dF}{dg} = \frac{\partial F}{\partial u} \frac{du}{dg} + \frac{\partial F}{\partial g} = 0 \implies \frac{du}{dg} = \left(\frac{\partial F}{\partial u} \right)^{-1} \frac{\partial F}{\partial g}. \quad (4)$$

We can then substitute (2b) and (4) into (3) to get a formula for the derivative:

$$\frac{d\mathcal{J}}{dg} = \frac{\partial \mathcal{J}}{\partial g} - \left(\frac{\partial F}{\partial g} \right)^* p. \quad (5)$$

Equation (5) illustrates the great advantage of using adjoint methods in optimization. In (3), we would need to compute the sensitivity of the state variables with respect to each control, which would lead to solving K systems of sensitivity equations (where K is the number of control variables, assuming (1) describes a finite-dimensional system, upon discretization of the original PDE). However, in (5), we only need to solve the adjoint equation once and then we can get all the components of the derivative of the cost function \mathcal{J} .

It should be noted that (5) is written in terms of directional derivatives. To retrieve the gradient, an appropriate inner product has to be chosen, resulting from a straightforward application of the Riesz representation theorem (see [3, 4] for the implications stemming from the choice of inner product).

Linear Algebra Formalism

In the case of the *differentiate-then-discretize* approach to adjoint methods, it is perhaps more intuitive to look at the problem from a linear algebra point of view, since the variables (\mathbf{u}, \mathbf{g}) are now discrete values approximated at each grid point and time step. We also denote by $\mathcal{J}^h(\mathbf{u}, \mathbf{g})$ the discretized cost function and by $F^h(\mathbf{u}, \mathbf{g})$ the discretized constraints, using any numerical scheme, in both space and time. We can look at a discrete equivalent of the derivative of the cost function from (3):

$$\frac{d\mathcal{J}^h}{d\mathbf{g}} = \frac{\partial \mathcal{J}^h}{\partial \mathbf{g}} + \frac{\partial \mathcal{J}^h}{\partial \mathbf{u}} \frac{d\mathbf{u}}{d\mathbf{g}}$$

and the discretized constraints from (4):

$$\frac{dF^h}{d\mathbf{g}} = \frac{\partial F^h}{\partial \mathbf{u}} \frac{d\mathbf{u}}{d\mathbf{g}} + \frac{\partial F^h}{\partial \mathbf{g}}.$$

The two equations can be formulated as:

$$\frac{d\mathcal{J}^h}{d\mathbf{g}} = \frac{\partial \mathcal{J}^h}{\partial \mathbf{g}} + \mathbf{h}^T \mathbf{v} \quad \text{with} \quad L\mathbf{v} = \mathbf{f}, \quad (6)$$

where we have renamed the variables as follows:

$$\begin{aligned} \mathbf{v} &= \frac{d\mathbf{u}}{d\mathbf{g}}, & \mathbf{h}^T &= \frac{\partial \mathcal{J}^h}{\partial \mathbf{u}}, \\ L &= \frac{\partial F^h}{\partial \mathbf{u}}, & \mathbf{f} &= -\frac{\partial F^h}{\partial \mathbf{g}}. \end{aligned}$$

From a linear algebra point of view, the above variables are simple matrices and vectors and we can simply introduce a new variable \mathbf{p} that will allow us to replace $\mathbf{h}^T \mathbf{v}$ with $\mathbf{p}^T \mathbf{f}$, where \mathbf{p} must satisfy $L^T \mathbf{p} = \mathbf{h}$. The fact that the two terms are indeed equivalent can be easily seen from:

$$\mathbf{p}^T \mathbf{f} = \mathbf{p}^T L\mathbf{v} = (L^T \mathbf{p})^T \mathbf{v} = \mathbf{h}^T \mathbf{v}.$$

A more thorough overview of the linear algebra viewpoint is given in [21]. This formalism is particularly appealing in the case of sensitivity and error analysis, where invoking the Lagrangian formalism, widely used in optimization, may seem too complex. The two methods are, of course, completely equivalent, but each has its strengths in particular contexts. As we will see, the Lagrangian viewpoint may be more intuitive when analyzing discrete numerical schemes (as it does not hide the complexity behind operators such as L), while the linear algebra viewpoint can be used in defining a modular, operator-based framework for the implementation of adjoint optimization methods (see [24]).

Burgers' Equation and Shocks

The model problem we will consider is the inviscid Burgers' equation:

$$\begin{cases} \partial_t u + \partial_x f(u) = 0, & (x, t) \in [a, b] \times [0, T], \\ u(x, 0) = g(x), & x \in [a, b], \end{cases} \quad (7)$$

where $f(u) = u^2/2$ and the equation is supplemented by appropriate boundary conditions on inflowing boundaries. For simplicity, we take the initial condition g as a control variable and a tracking-type cost functional:

$$\mathcal{J}(u, g) = \int_a^b G(u(T)) dx. \quad (8)$$

Using (2b), we derive the adjoint equations:

$$\begin{cases} -\partial_t p - u \partial_x p = 0, & (x, t) \in [a, b] \times [0, T], \\ p(x, T) = G'(u(T)), & x \in [a, b], \end{cases} \quad (9)$$

where p is the adjoint variable, as before. Given the fact that the Lagrangian is linear in p , the adjoint equations will themselves be linear PDEs. However, this formal derivation of the adjoint is done under strong continuity and differentiability hypotheses for all functionals and variables. Given the nonlinear nature of (7), shocks will develop for smooth initial datum at the break time:

$$T_b = \min_x \left(-\frac{1}{\partial_x u(x, 0)} \right),$$

so we can no longer rely on the previous results for $T > T_b$ (provided $T_b > 0$, of course). This case has been discussed in detail in [20] and more recently in [18, 19] and involves keeping track of the shock position as defined by the Rankine-Hugoniot conditions across the shock:

$$\dot{x}_s \llbracket u \rrbracket = \llbracket f(u) \rrbracket,$$

where \dot{x}_s is the shock velocity (thus x_s is its position) and $\llbracket \cdot \rrbracket$ denotes the jump in the given quantity across the shock. If we assume that the shock is present on a curve $\Gamma = (t, x_s(t))$, then the equations we have defined above remain valid for $\Omega \setminus \Gamma$ and a new set of equations has to be added to define the perturbation to the shock position given by the Rankine-Hugoniot condition. From [18], it is:

$$\dot{x}_s \llbracket u \rrbracket + \dot{x}_s \left[\tilde{u} + \tilde{x}_s \frac{\partial u}{\partial x} \right] - \left[u \tilde{u} + \tilde{x}_s \frac{\partial f(u)}{\partial x} \right] = 0, \quad (10)$$

which can be further reduced to the following evolution equation for the linearized shock position:

$$\frac{d}{dt} (\tilde{x}_s \llbracket u \rrbracket) = \llbracket (u - \dot{x}_s) \tilde{u} \rrbracket,$$

where \tilde{u} and \tilde{x}_s are small perturbations to the base state (u, x_s) .

The derivation above is largely based on the theory of generalized tangent vectors developed in [14] as a new form of variational calculus for such systems. This methodology is also described in [18, 20] and in [23], which proposes a new steepest descent method including the shock positions in the system. A very important point to be made is that, even if the state variables are discontinuous along the shock, the adjoint variable p in (9) has a uniform value along all characteristics leading backwards from the shock at position x_s [20].

A different formal approach is taken in [17], where the author has tried to contain the

amount of knowledge needed about the shock positions in formal convergence proofs. To this end, a new notion of *shift-differentiability* is defined for functions with moving discontinuities, which implies, under fairly general assumptions, the Fréchet-differentiability of tracking-type functionals as the one given by (8). Furthermore, [17] shows that entropy solutions to conservation laws, such as (7), are shift-differentiable under fairly general hypotheses, paving the way for a rigorous definition of the adjoint equations in the presence of shocks.

We also note that, for Burgers' equation, the adjoint equation is an advection equation with a discontinuous velocity. This case has been studied in [34] and [35], where it has been proven that there exist unique solutions, called *reversible solutions* for this type of equation in the space of local Borel measures $\mathcal{M}_{\text{loc}}(\mathbb{R})$. Extensions to the case of adjoint equations were proposed in [17] which can handle discontinuous end data, non-homogeneous right-hand sides, rarefactions waves and, most importantly, prove the differentiability for the cost functional.

III. Temporal Consistency

The interest of this paper lies in studying the convergence of discrete adjoint numerical schemes, i.e. schemes obtained by using the *discretize-then-differentiate* approach to adjoint optimization (see [3]). To give a proof of concept for this approach, we first discretize (7) using a classic Finite Volume method. The domain $\Omega = [a, b]$ is discretized into N cells:

$$T_i = [x_{i-\frac{1}{2}}, x_{i+\frac{1}{2}}]$$

centered at x_i with a uniform cell size Δx . By integrating over each space-time cell $T_i \times [t^m, t^{m+1}]$, we get the following update formula for the state variable u :

$$\begin{cases} u_i^{m+1} = u_i^m - \frac{\Delta t}{\Delta x} \left(f_{i+\frac{1}{2}}^m - f_{i-\frac{1}{2}}^m \right), \\ u_i^0 = g_i, \end{cases} \quad (11)$$

where the cell and face averaged variables are defined as:

$$\begin{aligned} u_i^m &= \frac{1}{\Delta x} \int_{T_i} u(x, t^m) \, dx, \\ f_{i-1/2}^m &= \frac{1}{\Delta t} \int_{t^m}^{t^{m+1}} f(u(x_{i-1/2}, t)) \, dt. \end{aligned}$$

We will now look at the modified Lax-Friedrichs scheme proposed in [18], for which the

flux may be written as:

$$f_{i-\frac{1}{2}}^m = \frac{1}{2}(f(u_i^m) + f(u_{i-1}^m)) - \frac{\epsilon}{\Delta x}(u_i^m - u_{i-1}^m), \quad (12)$$

where $\epsilon = \Delta x^\alpha$ and $\alpha \in (2/3, 1)$ is a grid-dependent parameter that will smear the shock over an increasing number of cells as $\Delta x \rightarrow 0$. The proposed scheme is stable under the CFL condition:

$$\max_i |u_i^m| \epsilon \frac{\Delta t}{\Delta x^2} \leq \frac{1}{2}.$$

Using these definitions, the update formula given in (11) describes a differentiable (with respect to u_i^m) finite volume scheme for (7) of order $\mathcal{O}(\epsilon)$. It is important to note that, in the continuous case, a formal analysis requires keeping track of the shock positions with additional equations like (10), but in the discrete case, the complexity can be sidestepped if the numerical scheme smears the shock appropriately [20].

If we denote by $\mathbf{u} = (u_i^m)$ and $\mathbf{g} = (g_i)$

$$g_i = \frac{1}{\Delta x} \int_{T_i} g(x) dx,$$

the solution vector and the control variable, respectively. The discretized cost functional (8) can be written as:

$$\mathcal{J}^h(\mathbf{u}, \mathbf{g}) = \sum_i \Delta x G(u_i^M).$$

Following the results from Section II, the discrete adjoint equations are:

$$\begin{cases} p_i^m = p_i^{m+1} + \frac{\Delta t}{\Delta x} (f_{i,+}^{*,m+1} + f_{i,-}^{*,m+1}), \\ p_i^M = G'(u_i^M), \end{cases} \quad (13)$$

where M denotes the total number of time steps and the “fluxes” are given by:

$$\begin{cases} f_{i,-}^{*,m+1} = \frac{1}{2}u_i^m(p_i^{m+1} - p_{i-1}^{m+1}) - \frac{\epsilon}{\Delta x}(p_i^{m+1} - p_{i-1}^{m+1}), \\ f_{i,+}^{*,m+1} = \frac{1}{2}u_i^m(p_{i+1}^{m+1} - p_i^{m+1}) + \frac{\epsilon}{\Delta x}(p_{i+1}^{m+1} - p_i^{m+1}). \end{cases} \quad (14)$$

We have written the discrete system in a very specific way so that it invites comparison to the continuous case (9). However, discretely, the adjoint equation is simply given by the transpose of the linearized discrete operator. In order to clearly see the fluxes, we consider the equations on a per-time step basis instead:

$$\mathbf{u}^{m+1} = \mathbf{u}^m - \mathcal{A}(\mathbf{u}^m), \quad (15)$$

where \mathcal{A} contains the flux term in (11). The adjoint equation is then simply obtain by linearizing \mathcal{A} around a reference state \mathbf{u}^m and transposing the operator to obtain:

$$\mathbf{p}^m = \mathbf{p}^{m+1} - \left(\frac{\partial \mathcal{A}}{\partial \mathbf{u}^m} \right)^T \mathbf{p}^{m+1}.$$

Using this formulation it is perhaps more intuitive to write the adjoint equation as follows:

$$p_i^m = p_i^{m+1} - \frac{\Delta t}{\Delta x} \left[\left(\frac{\partial f_{i-1/2}^m}{\partial u_i^m} \right) p_{i-1}^{m+1} + \left(\frac{\partial f_{i+1/2}^m}{\partial u_i^m} - \frac{\partial f_{i-1/2}^m}{\partial u_i^m} \right) p_i^{m+1} + \left(-\frac{\partial f_{i+1/2}^m}{\partial u_i^m} \right) p_{i+1}^{m+1} \right], \quad (16)$$

where it is obvious that the second term on the right-hand side is the result of a matrix-vector multiplication. In this very specific case, the operator \mathcal{A} only has 3 elements on row i at positions $(i-1, i, i+1)$ corresponding to the stencil of the numerical scheme, so we see only 3 terms in (16). This is a very generic formulation, as opposed to (14), where the fluxes have already been differentiated, with obvious extensions to schemes with wider stencils and more complicated flux formulæ.

It should be noted that, in the discrete case, no specific attention needs to be set on the differentiability and the presence of shocks since we are differentiating in \mathbb{R}^n . However, we do need to worry about the differentiability of the numerical scheme and, more importantly, the convergence to the continuous equations, which is itself a very complex issue. Numerical and formal proofs of convergence have been given in [18] for the modified Lax-Friedrichs scheme adopted here.

We will now briefly look at the convergence and the order of accuracy for the case of the modified Lax-Friedrichs scheme (11) and its adjoint (13). For testing purposes, we take a cost functional with $G(u) = \frac{1}{2}u^2$ and the following exact solution with a single shock at $x = 0$:

$$u(x, t) = \begin{cases} 1.5, & x < 0.5t, \\ -0.5, & x > 0.5t \end{cases} \quad (17)$$

and a known solution to the adjoint equation (9) for $T = 1$:

$$p(x, t) = \begin{cases} 1.5, & x < -1 + 1.5t, \\ 0.5, & -1 + 1.5t < x < 1 - 0.5t, \\ -0.5, & x > 1 + 0.5t, \end{cases} \quad (18)$$

where the middle state in the adjoint is computed from $\llbracket G(u) \rrbracket / \llbracket u \rrbracket$ (see [20]). We also take $T = 1.0$, $\Omega = [-1.5, 1.5]$, and a CFL of 0.9. A similar test has been performed in [22] for

the upwind scheme and very good convergence results were obtained. We can see in Table 1 that the forward scheme converges with the expected order α , while the adjoint equation converges with order $\alpha/2$. We have used the following discrete L_1 norm for the error estimates:

$$\|e_*\|_1 = \sum \Delta x |u_i^M - u(x, T)|,$$

which aggregates both time and space errors.

Table 1. L_1 error results for the state variable e_u and the adjoint variables e_p .

	128	256	512	Order
$\log(\ e_u\ _1) (\alpha = 0.999)$	-2.77028	-3.42418	-4.15565	0.999
$\log(\ e_p\ _1) (\alpha = 0.999)$	-1.13771	-1.49982	-1.85148	0.514
$\log(\ e_u\ _1) (\alpha = 0.9)$	-2.37230	-2.98675	-3.61683	0.897
$\log(\ e_p\ _1) (\alpha = 0.9)$	-0.91325	-1.21177	-1.52599	0.441
$\log(\ e_u\ _1) (\alpha = 0.8)$	-1.99073	-2.54112	-3.09571	0.797
$\log(\ e_p\ _1) (\alpha = 0.8)$	-0.72734	-0.96850	-1.24296	0.372

III.A. First Order Explicit Euler Time Integration

We now investigate the time consistency of the adjoint equations. Namely, in the adjoint fluxes (14), we have used the state variables at time t^m , while the adjoint variable was advancing backwards in time from t^{m+1} to t^m . This is not obvious from the continuous formulation and hidden beneath the linearized discrete operator L in (6). To better understand the problem, we will look at a scalar ODE of the form:

$$y'(t) = f(t),$$

which, discretized using an explicit forward Euler integration method, is:

$$\frac{y^{m+1} - y^m}{\Delta t} = f(t^m).$$

We can also write the above equation as $A\mathbf{y} = \mathbf{f}$. In the continuous case, the adjoint of ∂_t is $-\partial_t$. However, in the discrete case the time derivative operator A and its adjoint A^T are

given by:

$$A = \frac{1}{\Delta t} \begin{bmatrix} 1 & 0 & 0 & \cdots & 0 \\ -1 & 1 & 0 & \cdots & 0 \\ 0 & -1 & 1 & \cdots & 0 \\ \vdots & & \ddots & & \vdots \\ 0 & & -1 & 1 & 0 \\ 0 & \cdots & 0 & -1 & 1 \end{bmatrix} \implies A^T = \frac{1}{\Delta t} \begin{bmatrix} 1 & -1 & 0 & \cdots & 0 \\ 0 & 1 & -1 & \cdots & 0 \\ 0 & 0 & 1 & \cdots & 0 \\ \vdots & & \ddots & & \vdots \\ 0 & & 0 & 1 & -1 \\ 0 & \cdots & 0 & 0 & 1 \end{bmatrix}$$

We will now look at the m -th term of the dot products $\langle \mathbf{x}, A\mathbf{y} \rangle$ and $\langle A^T\mathbf{x}, \mathbf{y} \rangle$, where \mathbf{y} is our variable and \mathbf{x} its adjoint. We have:

$$\begin{cases} x^m \left(-\frac{1}{\Delta t} y^{m-1} + \frac{1}{\Delta t} y^m \right), \\ y^m \left(\frac{1}{\Delta t} x^m - \frac{1}{\Delta t} x^{m+1} \right), \end{cases} \iff \begin{cases} x^m \left(\frac{y^m - y^{m-1}}{\Delta t} \right), \\ y^m \left(-\frac{x^{m+1} - x^m}{\Delta t} \right), \end{cases}$$

which is also consistent with the property of the continuous operators. This equality shows that the m th term from $\langle A^T\mathbf{x}, \mathbf{y} \rangle$ matches the “state” variable y at time t^m with the adjoint variable x advancing backwards in time from t^{m+1} to t^m , as expected.

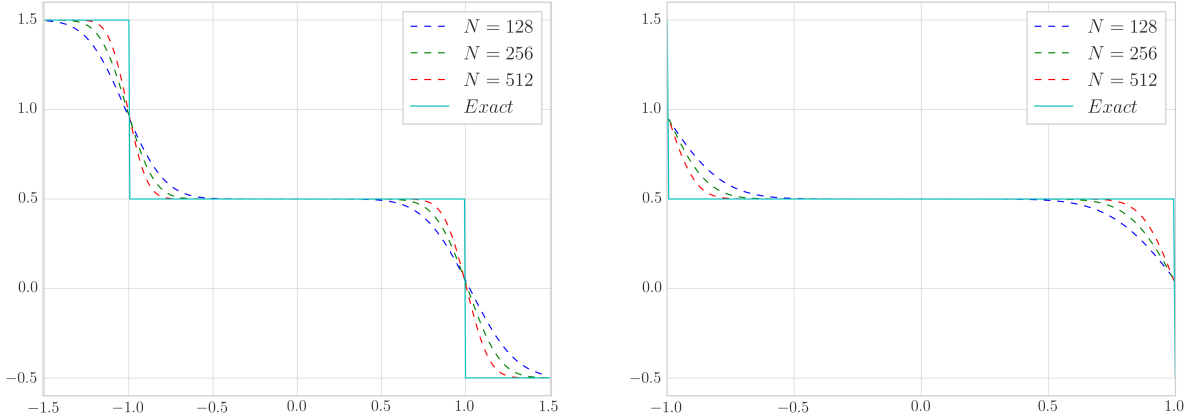


Figure 1. Adjoint solution at $t = 0$ for (18) (left) and a zoom around the shock position at $x = 0$ (right) with consistent time-stepping.

Figure 1 shows that the modified Lax-Friedrichs scheme with the consistent time advancement converges correctly to the exact adjoint solution. Note that this is not exactly the case for the upwind scheme in [22] where the solution seems to oscillate slightly around the exact solution. Figure 2 illustrates the results of the scheme using u_i^{m+1} in (14). The scheme no longer converges to the exact solution and the plateau is slightly below the exact

value. This is due to the inconsistent time integration scheme used.

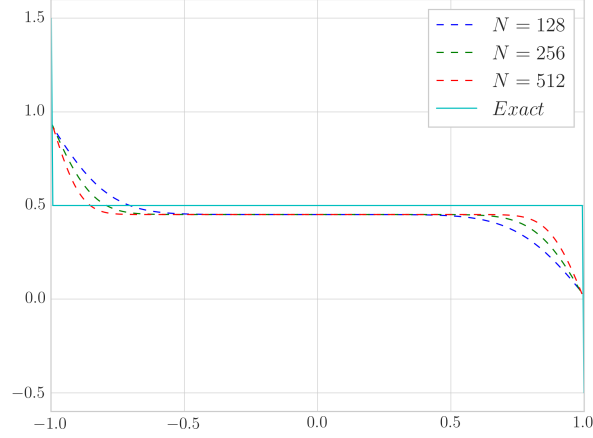


Figure 2. Adjoint solution at $t = 0$ for (18) zoomed around the shock position at $x = 0$.

III.B. Second-Order Runge-Kutta Time Integration

While the issues regarding time integration of the discrete adjoint are rather obvious for the explicit Euler method used above, they are more subtle for higher order methods, such as the Runge-Kutta family of methods. In this section we will analyze two second-order Runge-Kutta methods and their adjoints, one explicit and one implicit method. Generally, a time integrator $\phi_{\Delta t}$ has a classic definition of its adjoint [27]:

$$\phi_{\Delta t}^* = \phi_{-\Delta t}^{-1}, \quad (19)$$

i.e. the adjoint is the inverse of the forward method with a negative time step. Using this definition, we can deduce that any explicit scheme will have an implicit adjoint. This is the case for the results we have obtained with the explicit Euler scheme in the previous section, albeit in a slightly convoluted way. Specifically, if the original scheme is explicit, the adjoint scheme will be implicit when integrated forward in time, but explicit when integrated backwards in time (see [26] for how to reverse time in a Runge-Kutta method).

To take advantage of different time integration methods, we first write the semi-discrete variant of (7) as a coupled system of ODEs:

$$\frac{d\mathbf{u}}{dt} = \mathcal{A}(\mathbf{u}),$$

where \mathcal{A} is the same as in (15). The interdependence of the ODEs originates from the fact that \mathcal{A} contains a non-local discrete spatial derivative. We can write the system more

explicitly, for the case of the 3 cell stencil in the modified Lax-Friedrichs scheme, as:

$$\frac{du_i}{dt} = \mathcal{A}_i(u_{i-1}, u_i, u_{i+1}). \quad (20)$$

First we will look at the second-order explicit Runge-Kutta method known as Heun's method (or the explicit trapezoidal rule):

$$\begin{cases} \mathbf{u}^{m+1} = \mathbf{u}^m + \frac{\Delta t}{2}(\mathbf{k}_1^m + \mathbf{k}_2^m), \\ \mathbf{k}_1^m = \mathcal{A}(\mathbf{U}_1), & \text{where } \mathbf{U}_1 = \mathbf{u}^m, \\ \mathbf{k}_2^m = \mathcal{A}(\mathbf{U}_2), & \text{where } \mathbf{U}_2 = \mathbf{u}^m + \Delta t \mathbf{k}_1^m, \end{cases} \quad (21)$$

which corresponds to the Butcher tableau with $b_1 = b_2 = 1/2$, $c_1 = 0, c_2 = 1$, $a_{11} = a_{12} = a_{22} = 0$ and $a_{21} = 1$. To find the adjoint of this method, we will use the Lagrangian formalism where:

$$\begin{aligned} \mathcal{L}^h(\mathbf{u}, \mathbf{k}_1, \mathbf{k}_2, \mathbf{p}, \mathbf{l}_1, \mathbf{l}_2, \mathbf{g}) = & \mathcal{J}^h(\mathbf{u}, \mathbf{g}) - \sum_{m=0} < \mathbf{p}^{m+1}, \left(\mathbf{u}^{m+1} - \mathbf{u}^m - \frac{\Delta t}{2}(\mathbf{k}_1^m + \mathbf{k}_2^m) \right) > \\ & - \sum_{m=0} < \mathbf{l}_1^{m+1}, (\mathbf{k}_1^m - \mathcal{A}(\mathbf{U}_1)) > \\ & - \sum_{m=0} < \mathbf{l}_2^{m+1}, (\mathbf{k}_2^m - \mathcal{A}(\mathbf{U}_2)) >, \end{aligned}$$

where the intermediate steps \mathbf{k}_i are seen as independent variables with constraints enforced by the new adjoint variables \mathbf{l}_i . To find the adjoint Runge-Kutta scheme, we will differentiate the Lagrangian with respect to the state variables \mathbf{u}, \mathbf{k}_1 and \mathbf{k}_2 to obtain the following expressions for the gradients:

$$\begin{aligned} \frac{\partial \mathcal{L}^h}{\partial \mathbf{k}_1^m} &= \frac{\Delta t}{2} \mathbf{p}^{m+1} - \mathbf{l}_1^{m+1} + \Delta t \left(\frac{\partial \mathcal{A}}{\partial \mathbf{u}^m}(\mathbf{U}_2) \right)^T \mathbf{l}_2^{m+1} = 0, \\ \frac{\partial \mathcal{L}^h}{\partial \mathbf{k}_2^m} &= \frac{\Delta t}{2} \mathbf{p}^{m+1} - \mathbf{l}_2^{m+1} = 0, \\ \frac{\partial \mathcal{L}^h}{\partial \mathbf{u}^m} &= (-\mathbf{p}^m + \mathbf{p}^{m+1}) + \left(\frac{\partial \mathcal{A}}{\partial \mathbf{u}^m}(\mathbf{U}_1) \right)^T \mathbf{l}_1^{m+1} + \left(\frac{\partial \mathcal{A}}{\partial \mathbf{u}^m}(\mathbf{U}_2) \right)^T \mathbf{l}_2^{m+1} = 0. \end{aligned}$$

The adjoint system we have obtained is another explicit Runge-Kutta method integrated backwards in time with a Butcher tableau where the a_{ij} matrix of coefficients has been

transposed. The resulting system can be written as:

$$\begin{cases} \mathbf{p}^m = \mathbf{p}^{m+1} + \frac{\Delta t}{2}(\mathbf{l}_1^{m+1} + \mathbf{l}_2^{m+1}), \\ \mathbf{l}_1^{m+1} = \left(\frac{\partial \mathcal{A}}{\partial \mathbf{u}^m}(\mathbf{U}_1) \right)^T \mathbf{P}_1, & \text{where } \mathbf{P}_1 = \mathbf{p}^{m+1} + \Delta t \mathbf{l}_2^{m+1}, \\ \mathbf{l}_2^{m+1} = \left(\frac{\partial \mathcal{A}}{\partial \mathbf{u}^m}(\mathbf{U}_2) \right)^T \mathbf{P}_2, & \text{where } \mathbf{P}_2 = \mathbf{p}^{m+1}, \end{cases} \quad (22)$$

where we have redefined the original adjoint variables as follows:

$$\mathbf{l}_1^{m+1} \equiv \frac{2}{\Delta t} \left(\frac{\partial \mathcal{A}}{\partial \mathbf{u}^m}(\mathbf{U}_1) \right)^T \mathbf{l}_1^{m+1} \quad \text{and} \quad \mathbf{l}_2^{m+1} \equiv \frac{2}{\Delta t} \left(\frac{\partial \mathcal{A}}{\partial \mathbf{u}^m}(\mathbf{U}_2) \right)^T \mathbf{l}_2^{m+1}.$$

For general formulations of the adjoint of an arbitrary discrete s -stage Runge-Kutta method see [25, 26]. A very important property of the adjoint, as defined in [26], is that the order of the adjoint method is the same as that of the original method, even when the original method is explicit. The result we have obtained here agrees very well with the general formulation from [26].

For comparison with the adjoint method derived previously (22), we will use an implicit method defined using the methodology from [26], namely the implicit midpoint method. The implicit midpoint method is a 1-stage second-order symmetric Runge-Kutta defined as:

$$\begin{cases} \mathbf{u}^{m+1} = \mathbf{u}^m + \Delta t \mathbf{k}_1^m, \\ \mathbf{k}_1^m = \mathcal{A}(\mathbf{U}_1), & \text{where } \mathbf{U}_1 = \mathbf{u}^m + \frac{\Delta t}{2} \mathbf{k}_1^m, \end{cases} \quad (23)$$

and its adjoint is similarly given by:

$$\begin{cases} \mathbf{p}^m = \mathbf{p}^{m+1} + \Delta t \mathbf{l}_1^m, \\ \mathbf{l}_1^m = \left(\frac{\partial \mathcal{A}}{\partial \mathbf{u}^m}(\mathbf{U}_1) \right)^T \mathbf{P}_1, & \text{where } \mathbf{P}_1 = \mathbf{p}^{m+1} + \frac{\Delta t}{2} \mathbf{l}_1^m. \end{cases} \quad (24)$$

Table 2. Runge-Kutta: L_1 error log results for the adjoint variable p .

	128	256	512	Adjoint Order	Stat Order
Heun's Method	-1.04299	-1.39669	-1.74686	0.507	0.999
Implicit Midpoint Method	-1.04384	-1.39697	-1.74701	0.507	0.999

We are mainly interested in comparing the two methods in the context of time consistency.

We have seen in the previous section (and Figure 2) that an inconsistent time stepping method may compromise the convergence of the numerical approximation to the correct solution.

We will use the same modified Lax-Friedrichs scheme for the space discretization and the exact solution given by (18) with a CFL = 0.9 as before. We can see in Table 2 that the two methods are basically indistinguishable both in error and final order. Note that the order of the method remains ≈ 1 for the state equations and ≈ 0.5 for the adjoint since the space discretization dominates at order α . This is not a major issue because we are simply interested in the consistency and the convergence of the adjoint Runge-Kutta methods and not in improving the accuracy.

We can see the same results in Figure 3 where both methods still converge to the exact solution around the shock position $x = 0$ at time $t = 0$. Similar convergence issues as in Figure 2 appear if the state variable is used at the inconsistent time \mathbf{u}^{m+1} in the adjoint Runge-Kutta methods (22) and (24).

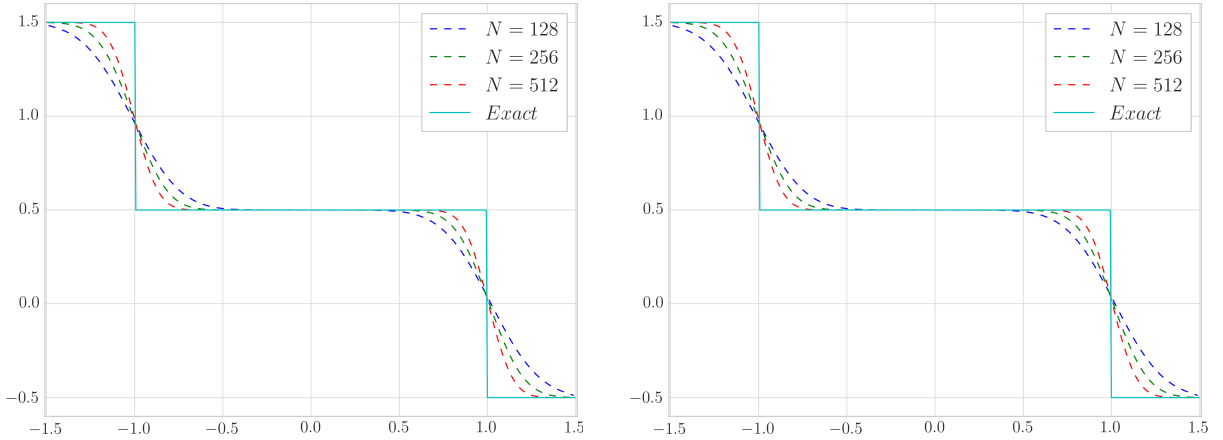


Figure 3. Adjoint solution at $t = 0$ for (18) using the explicit Heun's method (left) and the Implicit Midpoint method (right) with consistent time-stepping.

IV. Spatial Consistency

In this section we will investigate the spatial consistency of adjoint schemes and issues that may arise from incomplete differentiation, non-differentiable Riemann solvers, etc. For the purpose of this study we choose a high-order nonlinear numerical scheme based on flux limiters. Note that flux limited schemes (as well as any MUSCL scheme) are not proven to converge to the correct adjoint solution. This is because one of the main ingredients in convergence proofs regarding nonlinear conservation laws with shocks is Oleinik's One-Sided

Lipschitz Condition (OSLC):

$$\frac{u(x, t) - u(y, t)}{x - y} \leq \frac{1}{t}$$

and its discrete equivalent. See, for example, [34, 35, 23, 17] for general proofs that heavily involve the OSLC. The only limiter that is known to satisfy the OSLC is the **maxmod** limiter [28], which, unfortunately, does not remove spurious oscillations from the solution (specifically, it allows undershoots), rendering it unacceptable in practice. In [17], an iterative method is proposed to ensure that a given slope, initially limited with any commonly used limiter, is modified in such a way that the scheme satisfies the OSLC. However, this makes the limiter itself overly complicated (both implementation-wise and from a computation overhead point of view), thus, not practical. Even though there are no formal proofs, [29] suggests that TVD MUSCL schemes are bounded in Lip^+ , even though they are not monotonically decreasing, as required by the OSLC, leading to convergence in certain cases.

Given the remarks from [29] and the fact that flux limited schemes are among the most used nonlinear high-order schemes, we have adopted them for the analysis of spatial consistency. Flux limited schemes are constructed as a combination of a low-order monotone scheme and a high-order oscillatory scheme, with the limiter choosing between the two such that no spurious oscillations are introduced near discontinuities. More exactly, the fluxes from (11) are now given by:

$$f_{i-\frac{1}{2}}^m(u_i^m, u_{i-1}^m, s_{i-1/2}, r_{i-1/2}) = f_{i-\frac{1}{2}}^{LO} + \phi(r_{i-1/2}) (f_{i-\frac{1}{2}}^{HI} - f_{i-\frac{1}{2}}^{LO}), \quad (25)$$

where ϕ is known as a *flux limiter*. A common choice, adopted here, is to use the first-order *upwind* flux and the second-order *Lax-Wendroff* flux as our two fluxes:

$$\begin{cases} f_{i-\frac{1}{2}}^{LO} = (1 - s_{i-1/2})f(u_i^m) + s_{i-1/2}f(u_{i-1}^m), \\ f_{i-\frac{1}{2}}^{HI} = \frac{1}{2} \left([f(u_i^m) + f(u_{i-1}^m)] + \frac{\Delta t}{\Delta x} u_{i-\frac{1}{2}}^m [f(u_i^m) - f(u_{i-1}^m)] \right), \end{cases} \quad (26)$$

where $u_{i-1/2}^m = f'(u_{i-1}^m)$, if $u_i^m = u_{i-1}^m$, or the shock velocity otherwise, given by:

$$u_{i-1/2}^m = \frac{u_i^m + u_{i-1}^m}{2}$$

and $s_{i-1/2}$ is an upwinding coefficient, given by the continuous sigmoid:

$$s_{i-\frac{1}{2}} = \frac{1}{1 + \exp\left(-u_{i-1/2}^m/\delta\right)}, \quad \delta \ll 1. \quad (27)$$

We are now left with defining the flux limiter. For the purpose of this study, we will

consider a differentiable and non-differentiable flux limiter, namely the **van Albada** limiter and the **minmod** limiter, given by:

$$\phi_{\text{albada}}(r) = \frac{r^2 + r}{r + 1} \quad \text{and} \quad \phi_{\text{minmod}}(r) = \max(0, \min(1, r)),$$

where the slope ratio is given by:

$$r_{i-\frac{1}{2}} = (1 - s_{i-\frac{1}{2}}) \frac{u_{i+1}^m - u_i^m}{u_i^m - u_{i-1}^m} + s_{i-\frac{1}{2}} \frac{u_{i-1}^m - u_{i-2}^m}{u_i^m - u_{i-1}^m}. \quad (28)$$

This completely defines our scheme. We note that the van Albada limiter was selected to ensure the differentiability of the numerical scheme itself, with respect to u_i^m , so that it can be meaningfully linearized. Complete differentiability requires a differentiable upwinding function (in this case, a sigmoid) and a differentiable flux limiter (the van Leer limiter is also a good choice). For testing purposes, we have also defined a discontinuous limiter so that we may investigate its effect on the adjoint scheme. Using these definitions, the adjoint scheme can be defined exactly like in (13), but with different adjoint “fluxes”. We will investigate two separate flux formulæ: one for which we differentiate the flux limiter ϕ (referred to as *complete differentiation*) and one that assumes that the flux limiter is not a function of the state variables u_i^m and therefore removing the differentiability property (referred to as *incomplete differentiation*). A previous study [22] suggests that the discrepancies are expected to remain small. However, the tests in [22] have been performed on the more complicated 2D Euler equations and may hide some subtleties.

Generically, the main difference between the adjoint “fluxes” for the completely and incompletely differentiated schemes is the fact that they have a stencil of 5 cells and 3 cells, respectively. In the incompletely differentiated case, the fluxes are:

$$\begin{cases} f_{i,-}^{*,m+1} = \left[\frac{\partial f_{i-1/2}^m}{\partial u_i^m}(u_i^m, u_{i-1}^m) \right] (p_i^{m+1} - p_{i-1}^{m+1}), \\ f_{i,+}^{*,m+1} = \left[\frac{\partial f_{i+1/2}^m}{\partial u_i^m}(u_{i+1}^m, u_i^m) \right] (p_{i+1}^{m+1} - p_i^{m+1}), \end{cases}$$

where the fluxes are only functions of u_i^m , without taking into account the upwinding $s_{i-1/2}$

and the slope ration $r_{i-1/2}$, and the completely differentiated fluxes are:

$$\left\{ \begin{array}{l} f_{i,-}^{*,m+1} = \left[\frac{\partial f_{i-3/2}^m}{\partial u_i^m}(u_{i-1}^m, u_{i-2}^m, s_{i-3/2}, r_{i-3/2}) \right] (p_{i-1}^{m+1} - p_{i-2}^{m+1}) + \\ \left[\frac{\partial f_{i-1/2}^m}{\partial u_i^m}(u_i^m, u_{i-1}^m, s_{i-1/2}, r_{i-1/2}) \right] (p_i^{m+1} - p_{i-1}^{m+1}), \\ f_{i,+}^{*,m+1} = \left[\frac{\partial f_{i+1/2}^m}{\partial u_i^m}(u_{i+1}^m, u_i^m, s_{i+1/2}, r_{i+1/2}) \right] (p_{i+1}^{m+1} - p_i^{m+1}) + \\ \left[\frac{\partial f_{i+3/2}^m}{\partial u_i^m}(u_{i+1}^m, u_{i+2}^m, s_{i+3/2}, r_{i+3/2}) \right] (p_{i+2}^{m+1} - p_{i+1}^{m+1}), \end{array} \right.$$

where the fluxes, besides being functions of u_i^m , also depend on the upwinding function $s_{i-1/2}(u_i^m, u_{i-1}^m)$ (27) and the slope ratio $r_{i-1/2}(u_{i+1}^m, u_i^m, u_{i-1}^m, u_{i-2}^m)$ (28), which can be differentiated using the chain rule. Using the fluxes above, the adjoint scheme (13) is completely defined in both cases.

Complete Upwind Scheme

For a first test, we take the flux limiter $\phi \equiv 0$, which gives the classic first-order upwind scheme, and investigate the effect of the parameter δ in (27). The test case is the same simple scenario described in (17)-(18) with a CFL of 0.4.

The results can be seen in Table 3 for various values of δ . For values of $\delta \geq 1$, the upwind schemes degenerates to a centered (unstable) scheme, and the adjoint scheme becomes unstable for CFL 0.4. However, for values < 0.1 (even the discontinuous case of $\delta = 0$) there are no significant differences in convergence order and error. Results can also be seen in Figure 4a for $\delta = 0.001$ and are very similar in appearance to those obtained in [22]. Given these results, we expect the order to go to 0 as the grid is refined further since the scheme does not seem to converge.

Table 3. Upwind Scheme: L_1 error log results for the adjoint variable p .

	81	243	729	Adjoint Order	State Order
$\delta = 1.0$	-1.23692	-1.61394	-1.68173	0.202	1.000
$\delta = 0.1$	-1.12534	-1.80489	-1.78244	0.299	0.999
$\delta = 0.01$	-1.11337	-1.83637	-1.75990	0.294	0.999
$\delta = 0.001$	-1.11223	-1.80167	-1.75728	0.293	0.999
$\delta = 0.0$	-1.11223	-1.80161	-1.75728	0.293	0.999

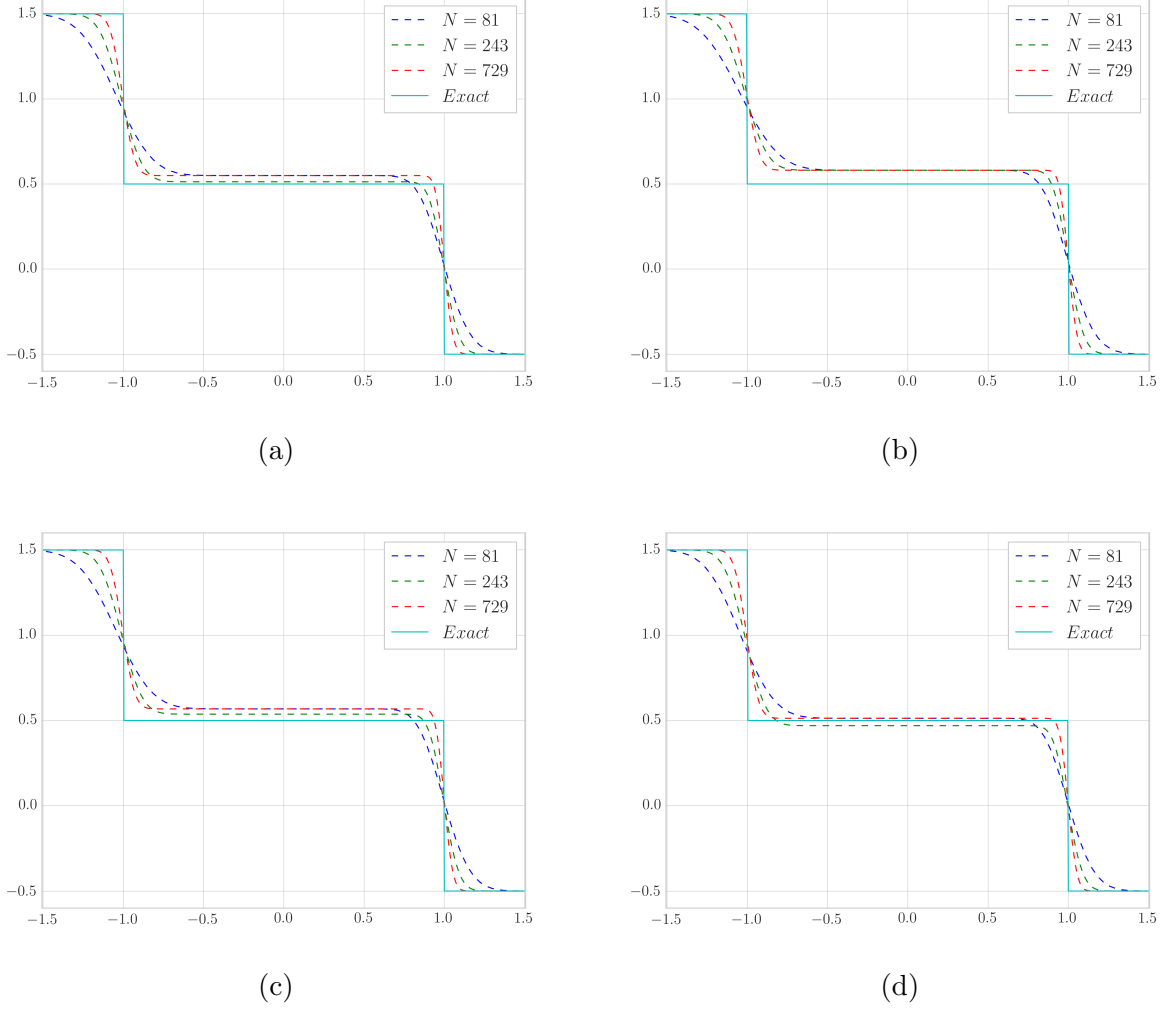


Figure 4. Convergence of the (a) upwind scheme, (b) a flux limited scheme with the minmod limiter, (c) incompletely differentiated scheme with the van Albada limiter and (d) completely differentiated scheme with the van Albada limiter for the test case (18) at time $t = 0$.

Incomplete MINMOD Scheme

Next, we consider the flux limited scheme with the `minmod` limiter. By construction, the `minmod` limiter is not differentiable, so we cannot fully differentiate the scheme, thus we must treat the flux limiter $\phi(r_i)$ as a constant.

We can see in Figure 4b (CFL = 0.3) that the flux limited scheme with the `minmod` limiter does not actually converge to the exact solution, even though it does seem to converge to another solution with very similar characteristics (i.e. continuous around the shock at $x = 0$). Furthermore, the results from Table 4 show, for various CFL conditions, the convergence order for the state and adjoint equations. The state equations converge at first-order, as expected, but the adjoint equations have an order that tends to 0 as the grid is refined (since it converges to the wrong solution).

Table 4. MINMOD: L_1 error log results for the adjoint variable p .

	81	243	729	Adjoint Order	State Order
CFL = 0.6	-1.44298	-1.97570	-2.45905	0.462	0.999
CFL = 0.3	-0.89866	-1.16698	-1.35208	0.206	0.999
CFL = 0.15	-0.81514	-1.07005	-1.24566	0.195	0.999

Complete and Incomplete van Albada Scheme

Finally, we will look at the effects of complete vs. incomplete differentiation of the flux functions in the differentiable flux limited scheme using the **van Albada** limiter.

Table 5. **van Albada**: L_1 error log results for the adjoint variable p .

	81	243	729	Adjoint Order	State Order
Complete. CFL = 0.4	-1.32960	-1.66087	-2.24946	0.418	0.999
Complete. CFL = 0.2	-1.14754	-1.54951	-1.89077	0.338	0.999
Incomplete. CFL = 0.4	-1.02991	-1.58054	-1.57674	0.248	0.999
Incomplete. CFL = 0.2	-0.89631	-1.18067	-1.38451	0.222	0.999

The results of this test can be seen in Table 5. It is clear that the incomplete differentiation of the **van Albada** limiter has essentially the same problem as we have seen with the **minmod** limiter and does not converge to the exact solution (see also Figure 4c). However, the completely differentiated scheme does not seem to behave any better. Finally, neither exhibits grid convergence properties at the intermediate state around the shock. In a way, we can consider this as validation of the results from [22] which also mention that complete vs. incomplete differentiation does not have a large impact on the end result.

Similar results can be seen in Table 6, where we have tested the **van Albada** limited scheme with the second-order Runge-Kutta method described in (21)-(22). The test, using a CFL of 0.5, has a slightly higher order for the tested grids, but the solution is not grid converged and there is still no significant difference between the completely and incompletely differentiated fluxes.

The same problem can be seen in all of the test cases we have seen in this section. As mentioned in [20], the adjoint numerical scheme basically needs to approximate the boundary condition:

$$\frac{\llbracket G(u) \rrbracket}{\llbracket u \rrbracket}$$

Table 6. van Albada with Heun’s time-stepping method: L_1 error log results for the adjoint variable p .

	81	243	729	Adjoint Order	State Order
Complete	-0.90772	-1.18163	-2.12105	0.552	0.869
Incomplete	-0.70418	-0.92006	-1.58714	0.401	0.869

at the shock and none of the schemes manage to capture it correctly for various grid sizes and CFL conditions. This can probably be best seen in Table 4 where for CFL 0.6 the scheme converges properly, but for CFL 0.3 the boundary condition is no longer correctly captured and the convergence suffers as an effect. We can, thus, conclude that it is relatively easy to come across a grid and time step combination for which the scheme converges to the wrong weak solution.

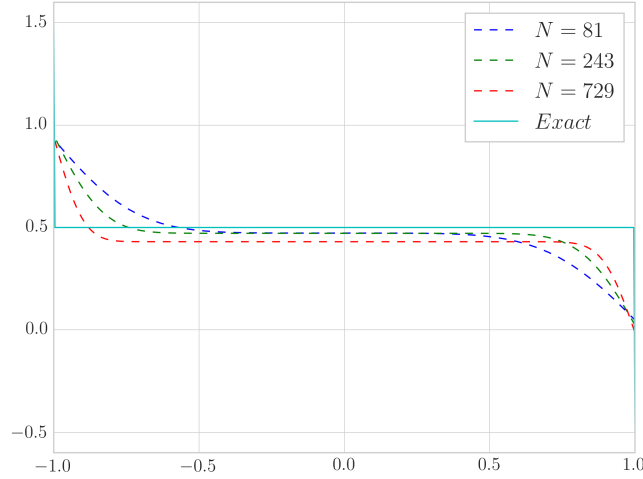


Figure 5. Adjoint solution at $t = 0$ for (18) using the modified Lax-Friedrichs scheme and the exact solution (17) for the state variable u^m .

This can even be seen with the modified Lax-Friedrichs scheme that normally converges to the correct solution. For a simple test, we will use the known exact solution (17) as input for the adjoint equation given by (13). Using the exact solution means that the shock is not smeared at all during the forward solve and the result can be clearly seen in Figure 5. So, even for a converging scheme as the modified Lax-Friedrichs scheme, if the shock is not sufficiently smeared during the forward solve, the adjoint will not converge to the correct solution for the same reasons as the flux limited schemes.

V. Hybrid Numerical Scheme

In this section we will attempt to construct a higher order scheme for Burgers' equation that also converges to the correct solution. Following well-established methodologies [30], the scheme we will look at is a *hybrid scheme* that uses a high-order flux limited scheme in smooth regions and the modified Lax-Friedrichs scheme around the shock. Using (25) and (12) we can construct a new scheme as follows:

$$f_{i-\frac{1}{2}}^m = \begin{cases} f_{i-\frac{1}{2}}^{LAX} = \frac{1}{2}(f(u_i^m) + f(u_{i-1}^m)) - \frac{\epsilon}{\Delta x}(u_i^m - u_{i-1}^m), & \rho_{i-1/2} > \rho, \\ f_{i-\frac{1}{2}}^{LIM} = f_{i-\frac{1}{2}}^{LO} + \phi(r_i) \left(f_{i-\frac{1}{2}}^{HI} - f_{i-\frac{1}{2}}^{LO} \right), & \rho_{i-1/2} \leq \rho, \end{cases} \quad (29)$$

where $\rho_{i-1/2}$ is a shock detector and $\rho > 0$ is a given threshold. We have chosen to use a variant of Harten's detector [30]:

$$\rho_{i-\frac{1}{2}} = \max(\rho_i, \rho_{i-1}),$$

where:

$$\rho_i = \frac{\left| \frac{|u_{i+\sigma}^m - u_i^m| - |u_i^m - u_{i-\sigma}^m|}{|u_{i+\sigma}^m - u_i^m| + |u_i^m - u_{i-\sigma}^m|} \right|^r}{},$$

where σ is a shift parameter and r is chosen such that the order of the detector $\rho_{i-1/2} = \mathcal{O}(\Delta x^r)$ is larger or equal to that of the high-order flux in the scheme (in this case, $r \geq 1$). Note that, since the detector $\rho_{i-1/2} \in [0, 1]$, Harten [30] originally defined the scheme as a convex combination between the two fluxes, while we have chosen to use it as a hard switch. Alternative detectors can be investigated, such as Jameson's detector [31], a simple detector from [22] that differentiates between shocks and rarefactions or more recent detectors [32] that can even distinguish between discontinuities and highly oscillatory solutions.

The adjoint scheme is obtained by differentiating the fluxes as in (16). However, given that both the shock detector and the scheme (29) are discontinuous, we will not differentiate them, so that the derivative is defined as follows:

$$\frac{\partial f_{i-1/2}^m}{\partial u_i^m} = \begin{cases} \frac{\partial f_{i-1/2}^{LAX}}{\partial u_i^m}, & \rho_{i-1/2} > \rho, \\ \frac{\partial f_{i-1/2}^{LIM}}{\partial u_i^m} & \rho_{i-1/2} \leq \rho. \end{cases}$$

We have seen in the previous section that complete vs. incomplete differentiation makes little difference when the scheme does not converge, so we do not expect the results to be affected. However, we still expect the adjoint scheme to converge to the correct intermediate state around the shock position because of the modified Lax-Friedrichs scheme. Using the

exact solution described in (17)-(18) with a CFL = 0.5, we will perform a number of tests on this new scheme to see how it performs compared to the others:

- Test 1:** Complete differentiation of the van Albada limiter with $\rho = 0.3, \sigma = 2$ and $r = 1$.
- Test 2:** Incomplete differentiation of the van Albada limiter with $\rho = 0.3, \sigma = 2$ and $r = 1$.
- Test 3:** Complete differentiation of the van Albada limiter with $\rho = 0.3, \sigma = 2$ and $r = 2$.
- Test 4:** Incomplete differentiation of the van Albada limiter with $\rho = 0.3, \sigma = 2$ and $r = 2$.
- Test 5:** Incomplete differentiation of the van Albada limiter with $\rho = 0.1, \sigma = 1$ and $r = 1$.
- Test 6:** Incomplete differentiation of the van Albada limiter with $\rho = 0.1, \sigma = 4$ and $r = 1$.
- Test 7:** Incomplete differentiation of the van Albada limiter with $\rho = 0.5, \sigma = 2$ and $r = 1$.
- Test 8:** Incomplete differentiation of the van Albada limiter with $\rho = 0.01, \sigma = 2$ and $r = 1$.

The results of the various tests can be seen in Table 7. We can see from Tests 1-4, that complete vs. incomplete differentiation has no effect on the scheme. However, given that the flux limited scheme operates mostly in constant regions, we can not draw conclusions from these tests. Furthermore, we can see that increasing the stencil using σ in Test 5-6 has a generally beneficial effect for convergence, while the overall order stays the same. Similar results can be seen when using a smaller threshold ρ , i.e. using the high-order flux less, in Test 7-8.

Overall, the convergence results in Table 7 are slightly better than those of the previously tested schemes, suggesting that better convergence for the adjoint equation is possible.

Table 7. Hybrid Scheme: L_1 error results for the adjoint variables e_p .

	81	243	729	Adjoint Order	State Order
Test 1	-0.94617	-1.66985	-2.33860	0.633	0.993
Test 2	-0.94792	-1.68200	-2.30667	0.618	0.993
Test 3	-0.86818	-1.38219	-1.81292	0.429	1.003
Test 4	-0.92688	-1.54892	-2.08032	0.524	1.003
Test 5	-0.95526	-1.69365	-2.35130	0.635	1.002
Test 6	-0.93081	-1.67549	-2.34335	0.642	1.002
Test 7	-0.92227	-1.64159	-2.22935	0.594	1.005
Test 8	-0.94667	-1.68759	-2.34862	0.638	1.002

To more thoroughly test the new scheme, we propose two new test cases, inspired by [20]. We use the same cost function as in (8) with $G(u) = u^5 - u$. First, we take a stationary shock problem:

$$u(x, t) = \begin{cases} 1, & x < \min(0.25 + t, 0.5), \\ \frac{x - 0.5}{t - 0.25}, & \min(0.25 + t, 0.5) < x < \max(0.75 - t, 0.5), \\ -1, & x > \max(0.75 - t, 0.5), \end{cases} \quad (30)$$

and the adjoint solution:

$$p(x, t) = \begin{cases} 4, & x < t, \\ 0, & t < x < 1 - t, \\ 4, & x > 1 - t. \end{cases} \quad (31)$$

The second test case is a moving shock problem with the exact solution:

$$u(x, t) = \begin{cases} 1, & x < \min(0.25 + t, 0.475 + 0.1t), \\ \frac{x - 0.5}{t - 0.25}, & \min(0.25 + t, 0.475 + 0.1t) < x < \max(0.7 - 0.8t, 0.475 + 0.1t), \\ -0.8, & x > \max(0.7 - 0.8t, 0.475 + 0.1t), \end{cases} \quad (32)$$

with the adjoint solution:

$$p(x, t) = \begin{cases} 4, & x < 0.025 + t, \\ -0.2624, & 0.025 + t < x < 0.925 - 0.8t, \\ 1.048, & x > 0.925 - 0.8t. \end{cases} \quad (33)$$

Test cases (30)-(31) and (32)-(33) have $T = 0.5$ and $\Omega = [0, 1]$. We can see the results in Figure 6 where the scheme is shown to converge in both cases.

The new hybrid scheme we have proposed seems to have marginally improved accuracy, while maintaining the same convergence qualities as the original modified Lax-Friedrichs scheme. However, it is very sensitive to the choice of parameters (ρ, σ) , that define the width around the shock where the Lax-Friedrichs scheme is used. We can see in the tests performed earlier that ρ has to be quite small for convergence, generally < 0.1 for the specific case of (18). For $\gtrsim 0.5$ the scheme no longer converges, although, in our tests, it does not deviate from the correct solution as much as the flux limited scheme (25) alone.

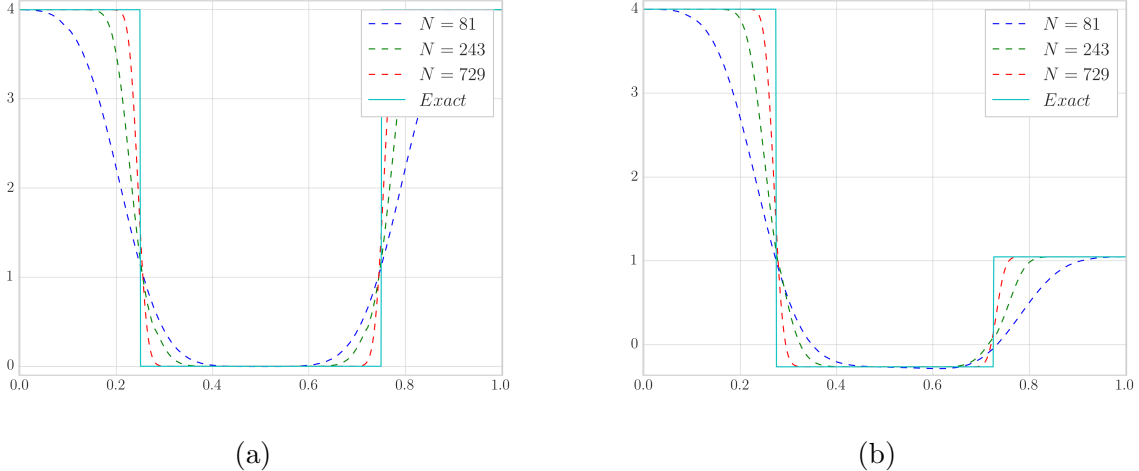


Figure 6. (a) Approximate solutions to (31) and (b) approximation solutions to (33) at $T = 0.25$.

VI. Conclusions

In this paper we have analyzed numerical schemes for scalar conservation laws in the presence of shocks. We have seen that a grid converged numerical scheme, like the modified Lax-Friedrichs scheme, needs to smear the shock across multiple cells as the domain is refined to correctly capture the state around the shock position in the adjoint solution. This was not the case for the flux limited schemes in Section IV and, as a result, none of them converged to the correct solution for all space and time discretizations. However, even in the case of non-converging numerical schemes, in most cases, the approximate solution was not far from the desired exact solution. We expect the error that occurs from incorrectly capturing the intermediate state to depend heavily on the magnitude of the shock. This implies that, for small shocks, a high-order, non-converging scheme may not incur a sizable error and may still provide sufficient resolution. While failure to converge may be a problem in sensitivity analysis, an iterative optimization algorithm may afford a slower convergence rate at the cost of higher accuracy in the numerical results.

While the error in convergence may prove manageable in certain scenarios, another error has been considered in this work, namely the error that comes with incompletely differentiating a highly nonlinear numerical scheme. We have repeatedly seen, for various limiters and various time stepping schemes, that incomplete differentiation also does not have much of an impact on the result. Specifically, the convergence properties do not improve when completely differentiating a nonlinear flux.

Finally, we have seen that a consistent time integration also has a significant impact on the convergence of the numerical scheme. Namely, if we were to discretize an adjoint obtained from the continuous state equations, it would be unclear at what time $t^* \in [t^m, t^{m+1}]$ the

state variables should be taken and what the impact is on the resulting scheme. This problem becomes completely clear in the discrete case where we are left with a single choice if we desire to be consistent with the discrete state equations. Higher order numerical integrators have also been investigated, both implicit and explicit, yielding favorable results. However, in our case, where the smooth regions are constant, higher order time integration did not have any impact on the resulting accuracy of the scheme.

References

- ¹O. Pironneau, *On Optimum Design in Fluid Mechanics*, Journal of Fluid Mechanics, Vol. 64, pp. 97-110, 1974.
- ²A. Jameson, *Aerodynamic Design via Control Theory*, Journal of Scientific Computing, Vol. 3, 1988.
- ³M. D. Gunzburger, *Perspectives in Flow Control and Optimization*, SIAM, 2003.
- ⁴A. Borzi, V. Schulz, *Computational Optimization of Systems Governed by Partial Differential Equations*, SIAM, 2012.
- ⁵M. Hinze, R. Pinnau, M. Ulbrich, S. Ulbrich, *Optimization with PDE Constraints*, Springer, 2008.
- ⁶J. L. Lions, *Optimal Control of Systems Governed by Partial Differential Equations*, Springer-Verlag, 1971.
- ⁷S. Zhang, X. Zhou, J. Ahlquist, I. M. Navon, J. G. Sela, *Use of Differentiable and Non-differentiable Optimization Algorithms for Variational Data Assimilation with Discontinuous Cost Functions*, Monthly Weather Review, Vol. 128, pp. 4031-4044, 2000.
- ⁸A. Iollo, M. D. Salas, *Optimum Transonic Airfoils Based on Euler Equations*, Computers and Fluids, Vol. 28, pp. 653-674, 1999.
- ⁹L. Huyse, R. M. Lewis, *Aerodynamic Shape Optimization of Two-dimensional Airfoils Under Uncertain Conditions*, Institute for Computer Applications in Science and Engineering Report, 2001.
- ¹⁰J. Glimm, E. Isaacson, D. Marchesin, O. McBryan, *Front Tracking for Hyperbolic Systems*, Advances in Applied Mathematics, Vol. 2, pp. 91-119, 1981.
- ¹¹T. Matsuzawa, M. Hafez, *Optimum Shape Design Using Adjoint Equations for Compressible Flows with Shock Waves*, AIAA Paper, 97-2078, 1997.
- ¹²A. Oyama, S. Obayashi, K. Nakahashi, T. Nakamura, *Transonic Wing Optimization Using Genetic Algorithms*, AIAA Paper, 97-1854, 1997.
- ¹³E. M. Cliff, M. Heinkenschloss, A. R. Shenov, *An Optimal Control Problem for Flows with Discontinuities*, Journal of Optimization Theory and Applications, Vol. 94, pp. 273-309, 1997.
- ¹⁴A. Bressan, A. Marson, *A Variational Calculus for Discontinuous Solutions of Systems of Conservation Laws*, Communications in Partial Differential Equations, Vol. 20, 1995.
- ¹⁵C. Homescu, I. M. Navon, *Optimal Control of Flow with Discontinuities*, Journal of Computational Physics, Vol. 187, pp. 660-682, 2003.
- ¹⁶C. Bardos, O. Pironneau, *Derivatives and Control in the Presence of Shocks*, Computational Fluid Dynamics Journal, pp. 383-392, 2003.
- ¹⁷S. Ulbrich, *Optimal Control of Nonlinear Hyperbolic Conservation Laws with Source Terms*, Habilitation Thesis, Zentrum Mathematik, Technische Universitat Munchen, Germany, 2001.

- ¹⁸M. B. Giles, S. Ulbrich, *Convergence of Linearized and Adjoint Approximations for Discontinuous Solutions of Conservation Laws. Part 1: Linearized Approximations and Linearized Output Functionals*, SIAM Journal of Numerical Analysis, Vol. 48, pp. 882-904, 2010.
- ¹⁹M. B. Giles, S. Ulbrich, *Convergence of Linearized and Adjoint Approximations for Discontinuous Solutions of Conservation Laws. Part 2: Adjoint Approximations and Extensions*, SIAM Journal of Numerical Analysis, Vol. 48, pp. 905-921, 2010.
- ²⁰M. B. Giles, *Discrete Adjoining Approximations with Shocks*, Proceedings of the Ninth International Conference on Hyperbolic Problems, pp.185-194, 2002.
- ²¹M. B. Giles, N. A. Pierce, *An Introduction to the Adjoint Approach to Design*, Flow, Turbulence and Combustion, Vol. 65, pp. 393-415, 2000.
- ²²F. Alauzet, O. Pironneau, *Continuous and Discrete Adjoints to the Euler Equations for Fluids*, International Journal for Numerical Methods in Fluids, Vol. 70, pp. 135-157, 2012.
- ²³C. Castro, F. Palacios, E. Zuazua, *An Alternating Descent Method for the Optimal Control of the Inviscid Burgers Equation in the Presence of Shocks*, Mathematical Models and Methods in Applied Science, Vol. 18, 2008.
- ²⁴M. Fosas de Pado, D. Sipp, P. J. Schmid, *Efficient Evaluation of the Direct and Adjoint Linearized Dynamics from Compressible Flow Solvers*, Journal of Computational Physics, Vol. 231, pp. 7739-755, 2012.
- ²⁵A. Sandu, *On the Properties of Runge-Kutta Discrete Adjoints*, Proceedings of the 6th international conference on Computational Science, Vol. IV, pp. 550-557, 2006.
- ²⁶W. W. Hager, *Runge-Kutta Methods in Optimal Control and the Transformed Adjoint System*, Numerische Mathematik, Vol. 87, pp. 247-282, 2000.
- ²⁷E. Hairer, G. Wanner, C. Lubich, *Geometric Numerical Integration*, Springer, 2006.
- ²⁸Y. Brenier, S. Osher, *The Discrete One-Sided Lipschitz Condition for Convex Scalar Conservation Laws*, SIAM Journal of Numerical Analysis, Vol. 25, pp. 8-23, 1988.
- ²⁹H. Nessyahu, E. Tadmor, T. Tassa, *The Convergence Rate of Godunov Type Schemes*, SIAM Journal of Numerical Analysis, Vol. 31, pp. 1-16, 1994.
- ³⁰A. Harten, *The Artificial Compression Method for Computation of Shocks and Contact Discontinuities: III. Self-Adjusting Hybrid Schemes*, Mathematics of Computation, Vol. 32, pp. 363-289, 1978.
- ³¹A. Jameson, W. Schmidt, E. Turkel, *Numerical Solutions of the Euler Equations by Finite Volume Methods Using Runge-Kutta Time-Stepping Schemes*, AIAA Paper 1259, 1981.
- ³²M. Oliveria, P. Lu, X. Liu, C. Liu, *Universal High Order Subroutine with New Shock Detector for Shock Boundary Layer Interaction*, AIAA Paper 2009-1139, 2009.
- ³³S. Nadarajah, A. Jameson, *A Comparison of the Continuous and Discrete Adjoint Approach to Automatic Aerodynamic Optimization*, AIAA Paper 2000-0667, 38th Aerospace Sciences Meeting and Exhibit, 2000.
- ³⁴F. Bouchut, F. James, *One-Dimensional Transport Equations with Discontinuous Coefficients* Nonlinear Analysis, Vol. 32, pp. 891-993, 1998.
- ³⁵L. Gosse, F. James, *Numerical Approximations of One-Dimensional Linear Conservation Equations with Discontinuous Coefficients*, Mathematics of Computation, Vol. 69, pp. 987-1015, 2000.